

Graphene CVD on Pd Substrates

A. Gutiérrez-Valdés^{1,2}, T. Zanatta-Martínez^{1,2}, and L.N. Serkovic-Loli²

¹Facultad de Ciencias, Universidad Nacional Autónoma de México, Ciudad Universitaria, Coyoacán 04510, México

²Instituto de Física, Universidad Nacional Autónoma de México, Ciudad Universitaria, Coyoacán 04510, México

Chemical vapour deposition (CVD) has become a standard method for the production of graphene in macroscopic quantities. In this work we implemented a protocol for graphene synthesis via CVD on palladium substrates. The obtained sample was analyzed through Raman Spectroscopy and Scanning Electron Microscopy (SEM) and the presence of monolayer and multilayer graphene was confirmed. This is the first instance of graphene deposition on Pd achieved in this laboratory, as such, we expect it serves as a starting point for future experiments using palladium as an alternative, and perhaps more effective for graphene growth than Cu or Ni.

Graphene | Palladium | CVD | SEM | Raman Spectroscopy

Author: agutierrez_v1796@ciencias.unam.mx

Introduction

As it is well known, graphene is an allotrope of carbon composed by a single (monolayer) or few layers of atoms (multilayer) arranged in a planar honeycomb lattice. Graphene exhibits many interesting properties, namely an extraordinarily good conductivity of heat and electricity, the strongest known Young modulus of any material (1 TPa)⁽¹⁾, great transparency and strong nonlinear diamagnetism.

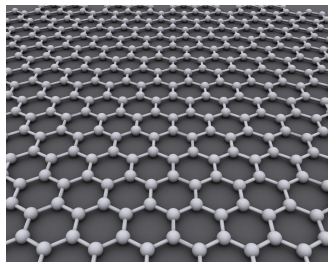


Fig. 1. Graphene chemical structure Note each carbon atom forms three covalent bonds which allows the fourth valence electron to be delocalized. Source: Wikimedia Commons

For the reasons stated above the production of graphene at large scales has become of great scientific and commercial challenge.

Graphene production through CVD. (2, 3)

CVD is a method used for fabricating materials that would otherwise be impossible to create. Generally, it involves flowing a precursor gas into an evacuated (low or high pressure), heated, chamber containing a solid object (called substrate) which becomes coated through chemical reactions with the gas. This allows the growth of thin films on the surface of the substrate while chemical byproducts are exhausted. Naturally, there are many variants depending on the desired application but one of the best studied methods for producing high quality graphene is known as low pressure

CVD. In this method a (chemically inert) quartz chamber is heated to temperatures ranging from 800 °C to 2000 °C while CH₄ is allowed to flow along with hydrogen and unreactive argon. A metallic substrate such as copper, nickel or palladium is placed inside the chamber and the synthesis is performed for variable amounts of time. A wide variety protocols (3, 4) have been established to produce different types of graphene which in turn possess diverse properties.

Raman Spectroscopy. The phenomenon of inelastic scattering was originally discovered in 1928 by C.V. Raman while studying light scattering by liquids with a mercury discharge lamp (5). Since the development of the laser in the 1960's, it has become a powerful analytic tool to determine the chemical composition of samples with great precision. Raman spectroscopy works on the principle of Raman (inelastic) scattering of monochromatic light (usually from a laser source in the visible or near IR) in a sample. This light excites molecular transitions in the material (roto-vibrational transitions) which result in an up or downshift of the scattered light. The energy shift allows us to access information about the vibrational modes of the system by measuring the shift (usually in wavenumbers per cm).

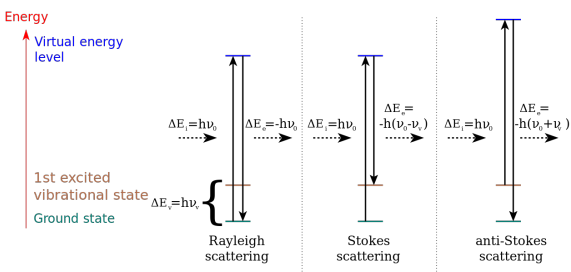


Fig. 2. Raman Scattering Model. Source: Wikimedia Commons

Graphene samples exhibit a characteristic Raman spectrum with 3 peaks which reveal information about its structure. According to (6) a high quality monolayer graphene sample should exhibit a sharp Lorentzian peak at around 2700 cm⁻¹ (known as the 2D peak) and a smaller (yet sharp as well) peak at 1587 cm⁻¹ (the G peak). Additionally, samples with a significant amount of defects might also display a third peak (D peak) at 1350 cm⁻¹ this is known as the disorder band and it should be as small as possible.

It is worth noting that these bands are calculated for graphene in Si substrates. While we are using the same parameters it serves only as a first approximation because our substrate is different and therefore must have slightly different resonances.

Empirically, the number of layers in a sample is found to correlate with a displacement in the G peak(6):

$$W_G = 1581.6 + \frac{11}{1+n^{8/5}} \quad (1)$$

Where W_G is the position of the G peak and n is the number of layers present in the sample. It is then possible to estimate n by simply substituting the measured value of W_G in

$$n = \left(\frac{11}{W_G - 1581.6} - 1 \right)^{5/8} \quad (2)$$

The presence of additional layers in the sample is confirmed by the FWHM of the 2D band which should be around 30 to 60 cm^{-1} in monolayer samples. If the peak is broader then the number of additional layers can be determined through a Lorentzian Multippeak fitting of the 2D peak, as shown below.

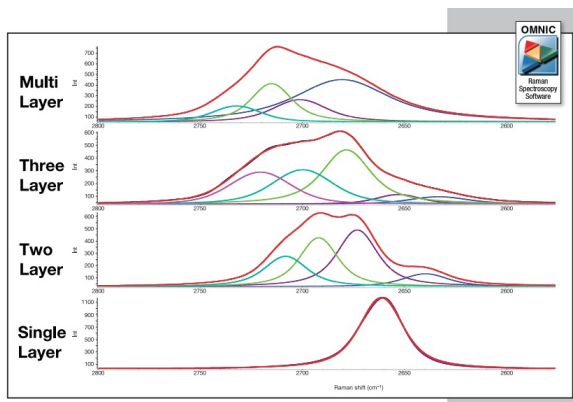


Fig. 3. 2D band exhibits distinct band shapes depending on the number of layers present. Source: Thermo Scientific.(6)

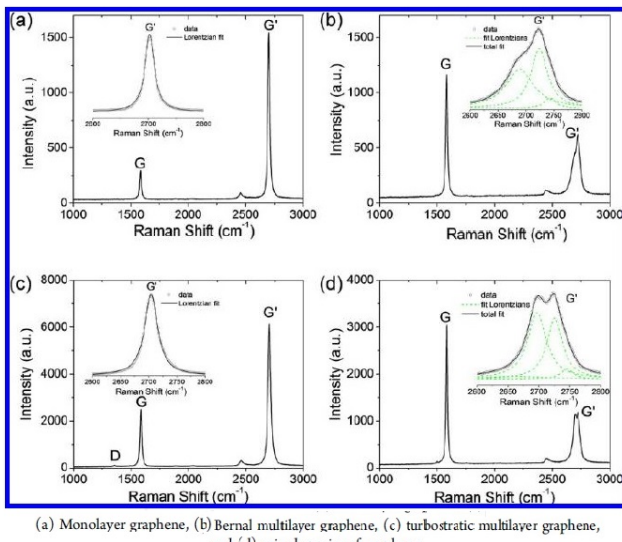


Fig. 4. Shapes of the 2D band and types of graphene as identified by Xiaohong, A. et al. (2012)(4)

A final indication of the presence of monolayer graphene is the ratio between the two main peaks, in that case a ratio $I_{2D}/I_G \approx 2$ should be expected.

Scanning Electron Microscopy (SEM). Electron microscopes utilize the scattering of a focused electron beam to probe samples with a resolution far beyond what is possible with optical microscopes (up to fractions of a nanometer)(7). The electrons interact with atoms in the sample, producing distinctive signals that contain information about the surface shape and chemical composition.

By the use of electromagnetic lenses (Lorentz force) the electron beam is focused and scanned in a raster pattern, and the position of the beam is combined in real time with the detected signal to produce an image. The image is generated by assigning a greyscale to each pixel which is proportional to the received secondary or back-scattered electrons(7). Complimentary information about the chemical composition of the sample may be obtained by a technique known as Energy-dispersive X-ray spectroscopy (EDS) in which the electron beam excites characteristic x-ray transitions in the sample and then the x-ray photons are detected with a photomultiplier.

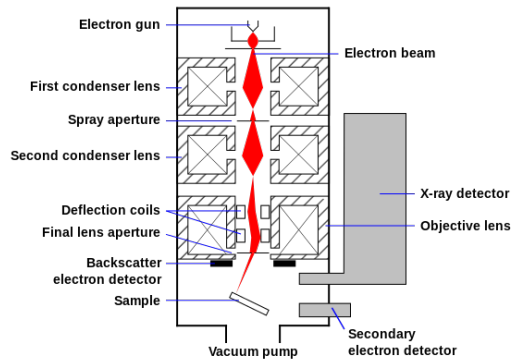


Fig. 5. Basic setup of a SEM. Source: Wikimedia Commons

The presence of graphene can be revealed through SEM due to the hexagonal symmetry of graphene crystals. The tell-tale sign is a structure with an angle of 120° as can be seen in the next figure:

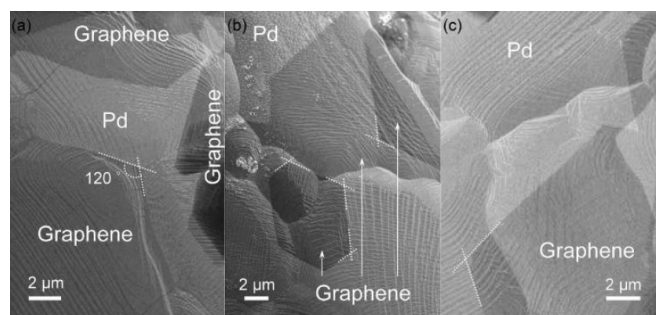


Fig. 6. Graphene observed by SEM as identified by Xiaohong, A. et al. (2012)(4)

Methods

The procedure for synthesizing graphene on Pd is described in the next section, it was based on the protocol implemented by Xiaohong, A et al. (2012)(4) since it is the only paper we found where an extensive analysis of graphene synthesis on Pd substrates was performed:

Before introducing the substrate to the vacuum chamber, it was cleansed with acetone and isopropyl alcohol for 5 minutes respectively and then dried with nitrogen gas to remove any remaining solvents.



Fig. 7. Chemicals used to clean the substrates

Graphene growth was achieved by a low-pressure CVD technique in a split tube furnace (model OTF-1200) with a quartz tube (10.16 cm in diameter). Pd substrates (Alfa Aesar), in the form of a 25 μm sheet, were cut to small pieces.

The sample was placed in the center of the furnace with a flow of hydrogen (60 sccm) and argon (30 sccm). The whole system was kept under vacuum (1.5 Torr), heated to $T = 950^\circ\text{C}$ (for the first and second batches, $T = 1000^\circ\text{C}$ for the third one), and kept at that temperature for 30 min in order to anneal the Pd. Then, methane gas (50 sccm) was introduced into the chamber for 15 minutes (20 seconds for the third batch).



Fig. 8. Experimental setup including the furnace and quartz tube

During the growth process, the pressure of the whole system was kept at 2 Torr. Finally the furnace was let to naturally cool down to room temperature under a pure argon flow.

SEM was performed on the samples with a JEOL JSM-7800F at 10 kV and 9.6×10^{-5} Pa, observing them at varying magnifications (1-100 μm).

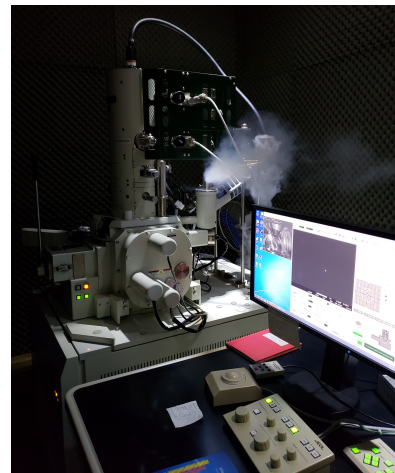


Fig. 9. Electron microscope used in the experiment

Raman Spectroscopy was performed with a Thermo Scientific DXR Raman instrument at a wavelength of 523 nm at 3 mW. A 50 μm pinhole was used and all samples were observed at 50x.



Fig. 10. Raman Microscope used in the experiment

Results & Discussion

Three different samples were prepared. The first two at $T=950^\circ\text{C}$ with a 15 min. methane flow were done in identical conditions except in two different days (we will call them sample 1 and 2). The last one (3) was done at $T=1000^\circ\text{C}$ with a flow of methane only 20 seconds long and several days later. Visual inspection of 1 and 2 clearly revealed a different tonality, 2 being the darker of the samples. SEM microscopy confirmed this difference as can be seen in the following images.

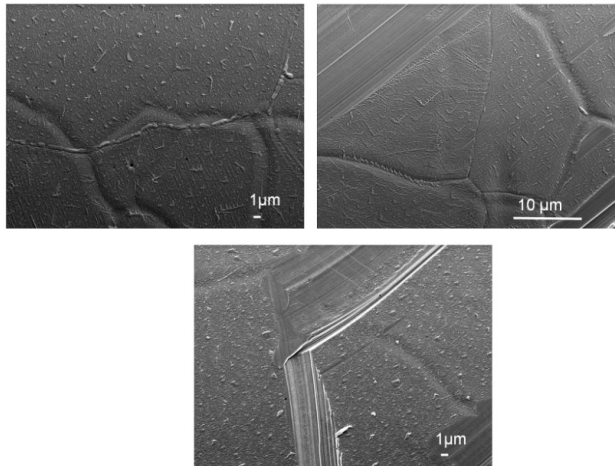


Fig. 11. SEM images of sample 1 at two different scales

No graphene was found on the first sample but these images demonstrate that the Pd substrate was properly annealed. Graphene is known⁽⁴⁾ to form near defects (ridges or corners) of the substrate.

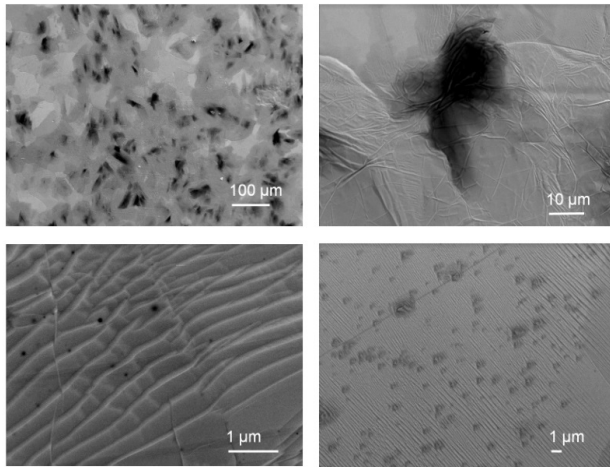


Fig. 12. SEM images of sample 2. Observe the contrasting dark islands and the variety of regions encountered.

In the second sample a wide variety of different regions were observed. At a scale of $100 \mu\text{m}$ carbon structures were clearly visible, contrasting from the lighter colored Pd background. Large blotches were formed which measure tens of microns. Smaller circular patches were also visible on the ridges of the substrate. Finally, a region which reminisces of a series of islands was also found.

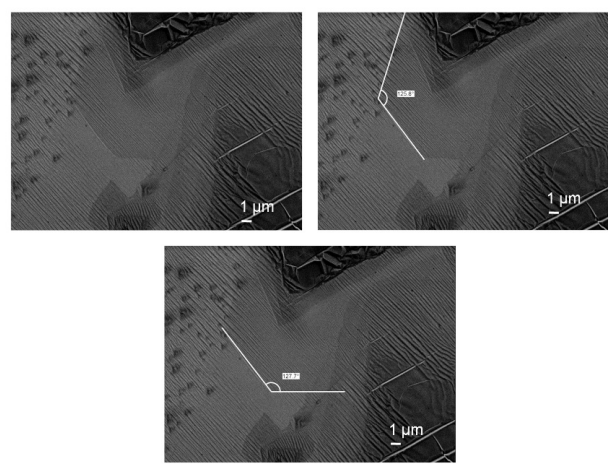


Fig. 13. SEM images of sample 2. Note the presence of sharp-cornered hexagonal structures.

In the vicinity of an island-like region an increasingly darker area was found which displayed the expected hexagonal symmetry. Sharp corners were observed although not at exactly 120° angles. This was taken to be evidence of the formation of, if not monolayer (because of the high opacity of the region) multilayer graphene. More conclusive evidence was provided by Raman Spectroscopy of the same sample.

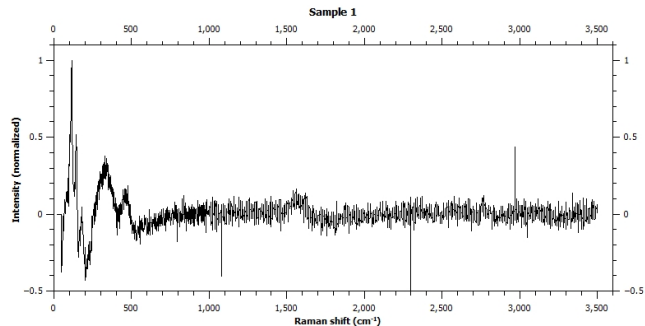


Fig. 14. Raman spectrum of sample 1. No clear lines were present.

Raman Spectra obtained for both sample 1 and 3 did not show the characteristic lines of graphene clearly and therefore were not analyzed any further. If anything, a small bump in the spectrum reveals the presence of bulk carbon.

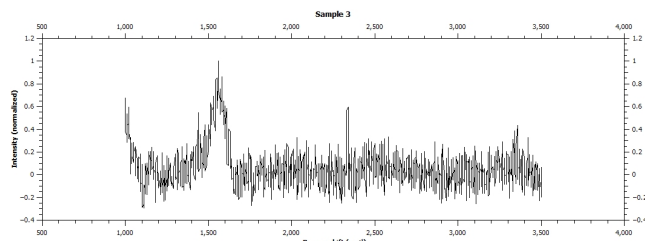


Fig. 15. Raman spectrum of sample 3. No lines were present.

Nevertheless, 5 spectra of the different regions observed in sample 2 were taken and clearly exhibited peaks at the G and 2D bands. A multipeak fit with Lorentzian curves was performed for each 2D band while a single Lorentzian curve was fitted to the G band.

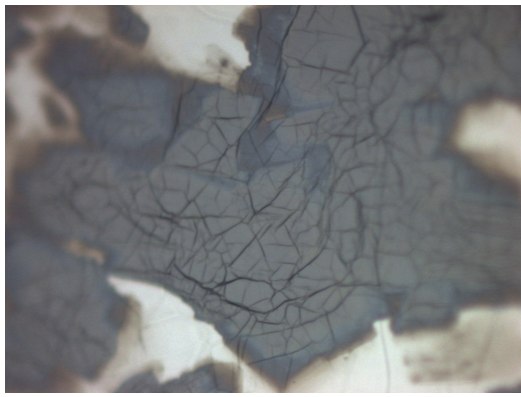


Fig. 16. Region 2a observed at 50x.

This region displays a significant dense, gray area with dark striations composed of carbon compounds, therefore we would expect to find mostly multilayer graphene.

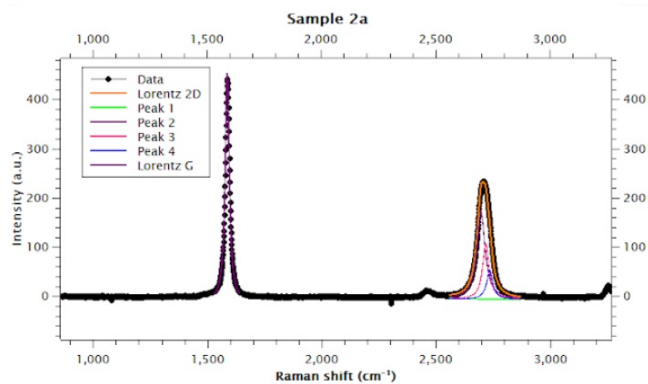


Fig. 17. Raman spectrum of sample 2a.

Table 1. Raman parameters for sample 2a

ω_{2D}	δ
2696.90	5.48
2716.16	3.38
2734.16	3.12
2737.52	9.56
ω_G	δ
1587.05	0.18

Table 2. Raman intensities for sample 2a

I_{2D}	I_G	I_{2D}/I_G	n
234.39	442.03	0.53	1.01

The G peak is centered around $\omega = 1587.05 \pm 0.18 \text{ cm}^{-1}$ very close from the 1587 cm^{-1} position expected in Si substrates.

Four Lorentzian peaks were used to fit the profile of the 2D band. The overall profile is consistent with multilayered Bernal graphene(4).



Fig. 18. Region 2b observed at 50x.

Sample 2b exhibits a lighter central section compared to sample 2a which possibly indicates less layers.

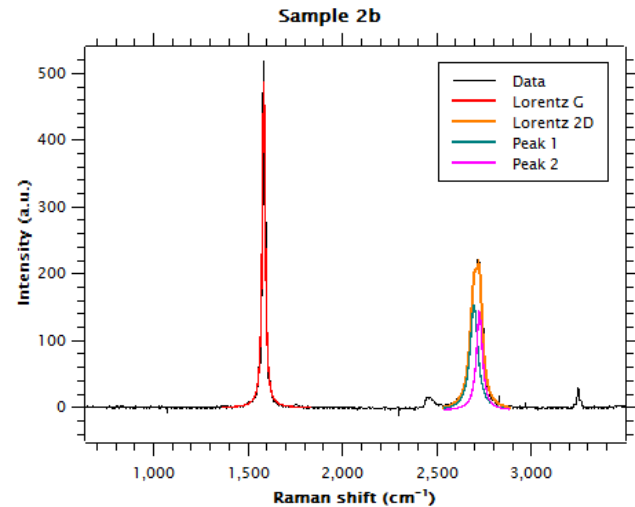


Fig. 19. Raman spectrum of sample 2b

In this case we observe a slight upshift in the G band and an inversion of the peaks in the 2D band with respect to the same peaks in sample 2a.

Table 3. Raman parameters of sample 2b

ω_{2D}	δ
2581.79	9.57
2700.10	0.31
2727.12	0.24
2745.19	0.74
ω_G	δ
1587.40	0.02

Table 4. Raman intensities for sample 2b

I_{2D}	I_G	I_{2D}/I_G	n
220.51	518.21	0.43	0.93

This profile is consistent with mixed-species multilayered graphene(4).

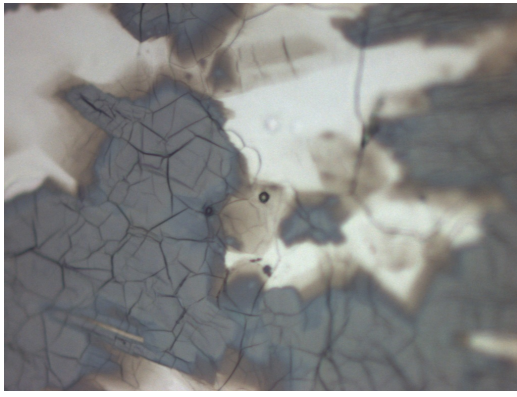


Fig. 20. Region 2c observed at 50x.

Region 2c features dark ring-like structures in the center, surrounded by a more transparent background.

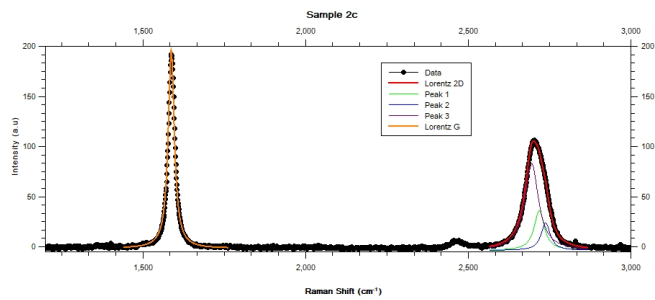


Fig. 21. Raman spectrum of sample 2c.

Table 5. Raman parameters of sample 2c.

ω_{2D}	δ
2719.12	0.83
2738.95	1.28
2696.09	0.61
ω_G	δ
1588.28	0.03

The upshift of the G peak once again goes in the opposite direction of what one would expect in Si substrates.

Table 6. Raman intensities for sample 2c

I_{2D}	I_G	I_{2D}/I_G	n
106.90	191.84	0.56	0.76

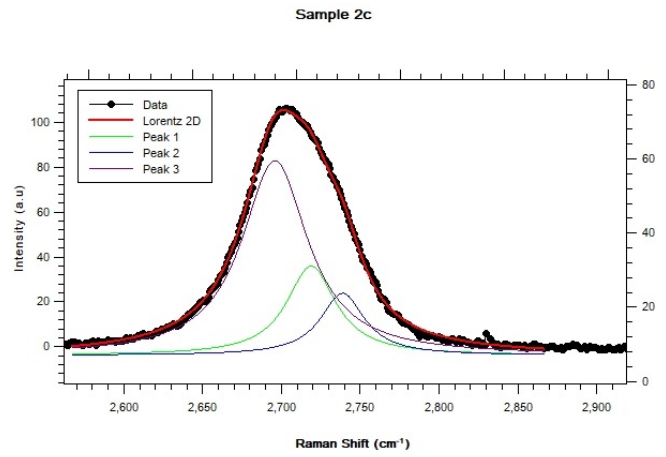


Fig. 22. Raman spectrum of sample 2c, focused on the 2D band.

It is interesting to note that in this case the 2D band required only 3 peaks for its correct fitting. Trying to adjust an additional peak did not improve the fitting. The broadened 2D peak points to Bernal multilayered graphene as the main component in this sample.

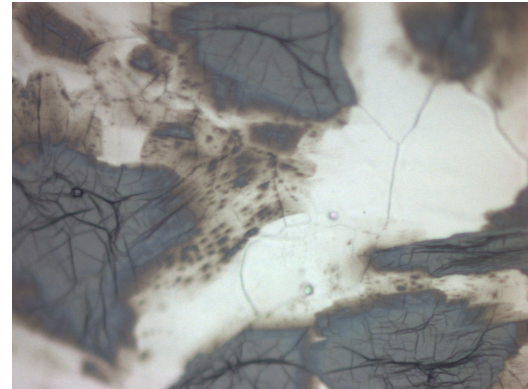


Fig. 23. Region 2d observed at 50x.

Region 2d has circular, denser structures embedded in a light grey area, which appear to be similar to region 2c but without the rings.

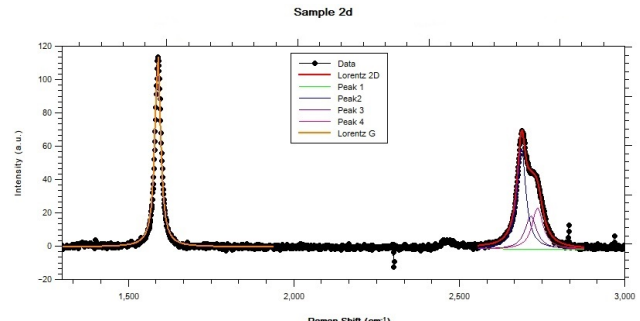


Fig. 24. Raman spectrum of sample 2d.

Table 7. Raman parameters for sample 2d

ω_{2D}	δ
2568.92	35.95
2689.21	0.32
2717.18	3.12
2737.52	2.44
ω_G	δ
1589.89	0.03

The G peak is noticeably upshifted when compared to the rest of the samples.

Table 8. Intensities and quotients sample 2d

I_{2D}	I_G	I_{2D}/I_G	n
69.00	113.41	0.61	0.50

This profile is again consistent with Bernal multilayer graphene. Perhaps of a thicker kind than sample 2a because of the width of the 2D peak ($FWHM \approx 70 \text{ cm}^{-1}$).

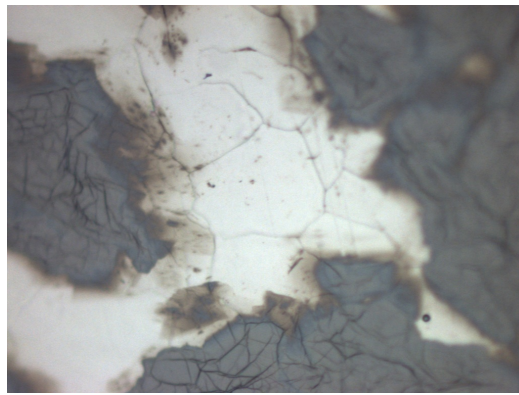


Fig. 25. Region 2e observed at 50x.

In sample 2e we observe a much lighter region which displays a gradient of gray tonalities. Raman was performed at the center of the image in a relatively transparent area with a small black spot.

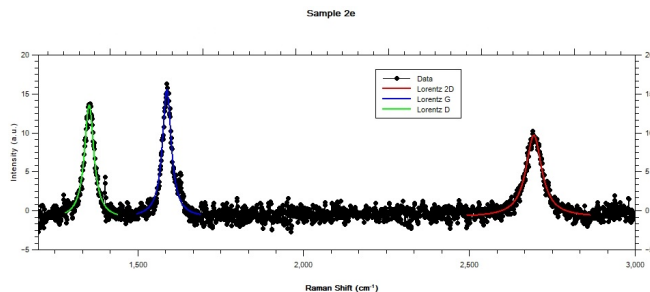


Fig. 26. Raman spectrum of the Sample 2e.

This spectrum is significantly different from the rest in many ways. The D line is not only visible but actually predominates over the 2D line. As it was already mentioned this reveals the presence of defects in the sample. Interestingly enough, the FWHM of the 2D line is about 50 cm^{-1} which corresponds to single layer graphene and is the smallest FWHM we measured. Therefore we can conclude the region contains both

monolayer and multilayer graphene (in the form of defects). This is the only time we encountered the former type.

Table 9. G band of spectrum 2e

ω_G	δG	I_G	n
1588.48	0.23	16.29	0.73

Table 10. 2D band of spectrum 2e

ω_{2D}	$\delta 2D$	I_{2D}	I_{2D}/I_G
2695.29	0.35	10.23	0.63

Table 11. D band of spectrum 2e

ω_D	δD	I_D
1354.27	1.03	13.74

Table 12. Approximate FWHM of the 2D band in sample 2

Sample	$\sim \text{FWHM } \omega_{2D} (\text{cm}^{-1})$
2a	65
2b	67
2c	73
2d	70
2e	50

From Raman analysis we can conclude that sample 2 is mostly made of multilayer graphene, particularly Bernal multilayer type with only a small percentage of monolayer graphene. It is also evident that formula (2) cannot effectively predict the thickness of graphene on Pd substrates and, in the absence of any theoretical model, analysis of the 2D band is essential. The quotient I_{2D}/I_G was never observed to be over 0.63 (in sample 2e), this strongly suggests the method should be refined if high quality monolayer graphene is to be obtained.

Conclusions

We have demonstrated an effective CVD method for graphene synthesis on palladium substrates but there are still many improvements to be made if it is to be refined. We are not sure why the technique did not work the first time. Since the conditions used for CVD were virtually the same both days, we suspect that the difference was due to *the first pancake rule*. Very few single-layer graphene was found on sample 2, this could be explained by the large deposition time used which tends to favor the formation of multilayer graphene. Even when rapid growth of graphene is reported⁽⁴⁾ at 1000°C (2 orders of magnitude faster than in Cu substrates) we did not observe the same rate and sample 3 did not form any graphene in 20 seconds. An approach such as the one followed by Xiaohong, An et al.⁽⁴⁾ could be used to determine the optimal temperature and CH_4 flow-time to grow mostly monolayer graphene in our setup.

ACKNOWLEDGEMENTS

The authors would like to thank Cristina Zorrilla (Raman Spectroscopy at Laboratorio de Materiales Avanzados) and Samuel Tehuacanero (SEM at Laboratorio Central de Microscopía) for their help with the analytical techniques used in this experiment.

Bibliography

1. Channgu L. et al. Measurement of the elastic properties and intrinsic strength of monolayer graphene. *Science*, 321(5887):385–388, 2008.
2. Creighton J.R. et al. Introduction to chemical vapor deposition (cvd). *ASM International*, page www.asminternational.org/documents/10192/1849770/ACFAA6E.pdf, 2001.
3. Wang S. et al. Synthesis of graphene on a polycrystalline co film by radio-frequency plasma-enhanced chemical vapour deposition. *Journal of Physics D*, 43(45):doi: 10.1007/s11434-012-5120-4, 2010.
4. Xiaohong A. et al. Large-area synthesis of graphene on palladium and their raman spectroscopy. *The Journal of Physical Chemistry C*, 116(31):doi:10.1021/jp301196u, 2012.
5. Raman C.V. A new radiation. *Indian Journal of Physics*, 2:387–398, 1928.
6. Wall M. The raman spectroscopy of graphene and the determination of layer thickness. *Thermo-Fisher Scientific*, Application Note: 52252:1–5, 2011.
7. Smith K.C. et al. The scanning electron microscope and its fields of application. *British Journal of Applied Physics*, 6(11):391–399, 1955.